TOXICOLOGICAL SCIENCES **92(1)**, 126–132 (2006)
doi:10.1093/toxsci/kfj182
Advance Access publication April 5, 2006

Tracheobronchial Particle Dose Considerations for *In Vitro* Toxicology Studies

Robert F. Phalen,*,[1] Michael J. Oldham,* and Andre E. Nel†

*Community and Environmental Medicine, School of Medicine, University of California, Irvine, California 92697-1825; and
†Department of Medicine, Division of Immunology and Allergy, University of California, Los Angeles, California 90095

Received January 10, 2006; accepted March 12, 2006

The purpose of this paper is to present a method for estimating particle doses that may be used to reconcile particle deposition doses used in *in vitro* toxicology studies with *in vivo* exposure levels. The focus is on the tracheobronchial (TB) tree of heavily exposed individuals. A review of the factors that influence inhaled particle deposition doses in environmental exposures leads to the identification of cases in which greater than average TB tree doses are received. Exercising individuals and those with chronic obstructive pulmonary disease not only inhale increased volumes of air but they also may have uneven ventilation that leads to greater than average particle deposition doses per unit of TB tree surface area. In addition, deposition hot spots, as occur at airway bifurcations, will greatly increase the particle exposures of target cells in the TB tree. Three particle exposure scenarios are proposed, and the average and local doses to the TB epithelium are calculated. When various factors that enhance particle doses (enhancement factors, or EFs) *in vivo* are considered, substantial particle doses may be justified for *in vitro* tissue culture studies that use TB target cells, such as epithelial cell cultures. The use of such EFs is intended to improve *in vitro* dosing with particles. Although the exposure of cells *in vitro* cannot fully replicate the complexity of *in vivo* exposures, it is possible to calculate toxicologically relevant doses that may define adverse health effects in potentially sensitive human populations. Local groups of TB cells in high-dose individuals are predicted to receive particle doses that are 3000–25,000 times higher than the doses averaged over the entire TB region.

Key Words: **particle deposition; *in vitro* doses; tracheobronchial tree; high-risk individuals; inhaled particles.**

Controlled laboratory toxicology studies with particulate pollutants are conducted using a variety of biological test systems, including humans, laboratory animals, isolated organs and tissues, cell cultures, subcellular organelles, and biomolecules. The usual objective is to obtain biologically relevant information that may predict adverse health effects in human individuals or populations. When living subjects are studied, the particles being investigated may be inhaled in order to simulate natural exposures. In this case, selection of realistic particle compositions, concentrations, and size distributions along with appropriate ventilation rates and exposure durations will provide useful data because proper doses will be delivered to intended target sites within the respiratory tract. Furthermore, the effects seen in inhalation exposures can generally be expected to represent those in unstudied populations because normal deposition, clearance, adsorption, translocation, distribution, metabolism, excretion, and toxicologic mechanisms will occur. However, when *ex vivo* studies are conducted, dose extrapolations are less certain because the particle exposures and mechanisms of injury occur under nonphysiological conditions.

When cell cultures are used as laboratory models, the influence of blood supply, neighboring cells and tissues, and many other biologically relevant factors is negated. Although extrapolation from studies that use cell cultures to intact living subjects will always be uncertain and artificial, relevant particle deposition doses should be delivered in order to maintain the applicability of such investigations. In this paper, information and guidance relevant to selecting doses of insoluble (actually slowly dissolving) particles for tracheobronchial (TB) tree epithelial cell cultures will be provided. The objective will be to mimic initial local doses expected to deposit *in vivo* on TB surfaces in humans to the extent practicable.

The efficiency with which aerosol particles deposit in the human TB region has been well studied in clinical settings, and the deposition mechanisms have been identified and sophisticated predictive mathematical models published (Brown *et al.*, 2005; CIIT, 2005; ICRP, 1994; NCRP, 1997). In human subjects, the TB deposition efficiency not only depends on the aerosol characteristics but also on the collection efficiency of

[1] To whom correspondence should be addressed at Community and Environmental Medicine, Room 100, Faculty Research Facility, North Campus, University of California, Irvine, CA 92697-1825. Fax: 949-824-4763, E-mail: rfphalen@uci.edu.

All the authors are members of the University of California, Los Angeles, Southern California Particle Center and Supersite.

Disclaimer: This work is not subject to the Environmental Protection Agency's peer and policy review; therefore, it does not necessarily reflect the views of the agency, and no official endorsement should be inferred.

the more proximal airways (nose, mouth, pharynx, and larynx), the nature of breathing (nasal vs. oral, tidal volume, and frequency), and individual differences in TB anatomy, both in normal individuals and diseased patients (Bennett *et al.*, 1997; Heyder *et al.*, 1982; Kim and Kang, 1997; Lippmann, 1977; and others). In general, resting normal individuals have a more even distribution of airflow and inhaled particle deposition in the respiratory tract in comparison to diseased individuals (Bennett and Zeman, 2004; Bennett *et al.*, 1997; Chalupa *et al.*, 2004; Sweeney *et al.*, 1995). Because the primary deposition mechanisms of inertial impaction, sedimentation, and diffusion that cause particles to contact airway walls are known, reliable computer programs for predicting such deposition in humans are available. Two such models currently in wide use are those of (1) the International Commission on Radiological Protection, called LUDEP (ICRP, 1994) and (2) the National Institute for Public Health and the Environment in collaboration with the CIIT Centers for Health (CIIT, 2005), called MPPD1 (Brown *et al.*, 2005). Although, as expected, each computational model yields somewhat different deposition efficiencies, each one may be used to predict regional particle deposition efficiencies in normal humans. For the nonaerosol scientist, MPPD1 is recommended, as it is available free of charge from CIIT (2005), is user friendly, and allows the user to input airborne concentrations, specific particle sizes, dispersions and concentrations, breathing characteristics, airway sizes (based on subject age), and other pertinent information. These computational models provide ''averaged'' deposition doses for the whole lung, TB or other anatomical region, specific lung lobes and in some cases each TB generation, but local deposition ''hot spots'' (areas of high deposition in relation to surrounding surfaces) are not modeled. Use of these models assumes that all cells in a given airway will receive the same particle deposition dose, which will underestimate the local doses delivered to cells located in certain areas, such as carinas (which are flow dividers or bifurcation regions) in the TB region.

There is abundant evidence that the deposition of inhaled particles is highly nonuniform within the respiratory tract. Such evidence initially came from bench-top particle deposition studies in hollow models representing airways (Bell and Friedlander, 1973; Churg and Vedal, 1996; Cohen *et al.*, 1988; Martonen *et al.*, 1987; Oldham *et al.*, 2000; Schlesinger *et al.*, 1982). Additional evidence for local high particle deposition has been provided by the examination of actual lung samples (Ishikawa *et al.*, 1994; Kaye *et al.*, 2000; Segal *et al.*, 2000) and by computational fluid dynamic (CFD) models that account for the effects of local airflows and anatomical detail (Balásházy and Hofmann, 1993; Balásházy *et al.*, 1999, 2003; Broday, 2004; Gradón and Orlicki, 1990; Heistracher and Hofmann, 1997; Hofmann *et al.*, 1996, 2000; Nowak *et al.*, 2003; Zhang *et al.*, 2005). The nonuniformity of CFD-predicted particle deposition is striking, which implies that some groups of epithelial cells receive initial particle doses that are not well represented by the non-CFD computational models. Thus, the CFD model predictions of local high-dose regions appear to represent what actually occurs for a large range of inhaled particle sizes (Ishikawa *et al.*, 1994; Kaye *et al.*, 2000; Oldham *et al.*, 2000). Such high-dose regions, or hot spots, are specified by local enhancement factors (EFs) that depend on the size of the region under consideration (sometimes called the patch size). In general, the smaller the patch size, at the apex of a bifurcation, the larger the EF (Balásházy *et al.*, 2003).

MATERIALS AND METHODS

Scenario 1. In order to estimate the TB epithelial surface doses for environmental exposures of humans, several particle exposure/deposition scenarios are examined. The first scenario is that of an average resting (nose breathing) adult who has no respiratory disease. To further simplify, only the TB airways region and the surface-averaged particle deposition (e.g., μg of particles/cm^2 of airway surface) will be considered. The average adult is assumed to have a body mass of 70 kg, a ventilation of 6 l/min, and the simplified TB anatomy of Yeh and Schum (1980). The TB region has an assumed surface area contacting the air of 2471 cm^2 (Mercer *et al.*, 1994). To estimate the initial deposition of particles, MPPD1 is used over a limited particle size range. Three inhaled particle aerodynamic diameters will be considered: 1, 2, and 5 μm. (Aerodynamic diameter is defined as the physical diameter of a smooth spherical particle of specific gravity 1.0 that has the same terminal settling velocity in still air, under standard conditions, as the particle in question.) For nasal breathing and the particle diameters selected, 1, 2, and 5 μm, the MPPD1 model gives resting adult TB deposition efficiencies (fraction of the particles inhaled) of 0.059, 0.086, and 0.116, respectively. The deposition calculations can also be used to provide averaged surface depositions/cm^2 of the TB region. These surface doses admittedly will not represent the effects of uneven particle deposition due to anatomical features (such as bifurcation zones) or the uneven distribution of airflow that may occur within the TB region.

Scenario 2. The second particle deposition scenario will take into account the effect of areas of high local particle deposition, i.e., deposition hot spots. Such hot spots have been successfully modeled for 1- to 5-μm-diameter particles using CFD computer codes by several investigators (Balásházy *et al.*, 1999, 2003; Hofmann *et al.*, 1996; Oldham *et al.*, 2000; Zhang *et al.*, 2005). The increased local particle deposition is quantified by calculation of the EF, which is the ratio of particle deposition in the local region of interest to that averaged over the entire airway. The EF will depend on several factors including the shape, location and size of the local region (e.g., a 0.1 × 0.1-mm patch in the center of a bifurcation), the airflow rate (e.g., rest vs. exercise), and the particle size. All of these parameters are conveniently presented by Balásházy *et al.* (1999, 2003); hence, their values are used in our dosimetry calculations for Scenario 2. EFs will be combined with other factors that increase particle doses that are described in Scenario 3.

Scenario 3. The third particle deposition scenario will take into account several factors that further enhance the total and local depositions of inhaled particles. Such factors include physical exercise (e.g., producing a minute ventilation of about 30 l), oral breathing (which bypasses the filtering efficiency of the nose), the presence of lung disease (which can produce highly uneven distribution of inhaled air), unfavorable airway geometry (which enhances particle deposition in the TB region and is observed in the normal population), and proximity to a source of particles (e.g., being exposed close to a busy highway or industrial source). These factors can be considered to define potentially high-risk individuals from the standpoint of increased doses to regions of the TB airways. Although the presence of high local-dose regions in the respiratory tract *per se* may not always increase risk, the principle of dose-response implies

that in many cases the risk will be increased. Scenario 3 represents the high-dose/high-risk individuals in the population.

Physical exercise both delivers more particles to the respiratory tract per unit time and alters the deposition efficiencies of particle deposition within each region of the respiratory tract (CIIT, 2005; ICRP, 1994). For the particle diameters of interest, 1, 2, and 5 μm, MPPD1 predicts TB region deposition efficiencies during 30-l/min (45 × 667 ml breaths/min) ventilation of 0.041, 0.032, and 0.023, respectively, for nasal breathing. For oral breathing at this level of ventilation, the deposition efficiencies of the three particle diameters are 0.054, 0.070, and 0.193, respectively. The TB deposition is larger in oral breathing because the nose is more efficient than the mouth in collecting particles. Although the TB deposition efficiencies in exercise are not always larger than those at rest, they must be multiplied by the increased rate of intake of air, which is five times above that at rest (30 vs. 6 l/min) for our scenario. Therefore, the TB depositions per unit time of particles during exercise at 30 l/min with oral breathing for 1, 2, and 5 μm particles are 0.270, 0.350, and 0.965, respectively, which are significantly larger than those predicted for the first scenario (resting, nasal breathing normal adult).

The presence of lung disease can significantly alter the doses of inhaled particles in many ways (increased deposition efficiency, less even distribution of inhaled air, and decreased particle clearance rates). The strongest quantification is available for chronic obstructive pulmonary disease (COPD) because it has been the most thoroughly studied. Bennett (2000) and Bennett *et al.* (1997) found that for 2.5-μm-diameter particles, total deposition was increased by a factor of 1.5 over normal individuals in 13 COPD patients. In addition, the COPD patients had an increased volume of ventilation that was 50% greater than that of normal individuals at rest. Two of the 13 patients had particle deposition efficiencies 2.5 times that of the normal group, and when increased ventilation was simultaneously considered, three COPD subjects had particle deposition rates that were four times greater than those for normal individuals. Considering these data, we will conservatively use a resting TB deposition EF of 2 to represent the anatomy effect in COPD patients for each particle aerodynamic diameter (1, 2, and 5 μm). With respect to uneven airflow distribution, it is difficult to find quantitative data in COPD patients, although the ventilation is assumed to be very uneven (Churg and Vedal, 1996; Kaye *et al.*, 2000; Segal *et al.*, 2002). Sweeney *et al.* (1995) measured an "evenness index" in bronchitic rats using radiolabeled particles. The evenness index data implied that only 55% of the lung volume was ventilated. Miller *et al.* (1995) discussed uneven ventilation in humans with severe COPD and noted that most of the ventilation is limited to one-fourth of the lung. Thus, we assume that severe COPD humans only ventilate 50% of their lungs. This implies that the surface doses in ventilated portions of the lungs would be increased by an additional factor of 2. Combining this factor with the factor of 2 for increased total deposition produces an increased TB surface deposition dose of 4 over that of healthy adults.

Another factor that enhances local particle doses over that of the average person is the effect of variations in airway geometry and ventilation on particle deposition in human populations. Individuals who have unusual particle deposition–related features may be at greater risk from inhaling particles. Studies of particle deposition in clinical settings show great variability in particle deposition. Using data summarized by Lippmann (1977) for TB deposition in nonsmokers, the SD for 5 μm particles inhaled at rest is 50% of the mean value. Therefore, the TB dose enhancement factor (DEF) associated with having unfavorable anatomy/physiology will be taken as 2; i.e., the TB surface doses are doubled in such individuals. In COPD patients, this factor was previously considered in the TB deposition EF.

It is well known that in environmental situations, some individuals' exposure will be better represented by the stationary air quality monitors than will others (Adgate *et al.*, 2002; Zhu *et al.*, 2002). Air quality monitors are usually "centrally located," i.e., they are placed to provide average population exposures, as opposed to individual exposures. Heterogeneity of particle exposures is produced by the location of the subjects in relation to local sources and the local environmental circumstance (e.g., outdoors vs. indoors). Adgate *et al.* (2002) reported the range of exposures in Minneapolis-St. Paul, MN, to particles 2.5-μm-diameter and smaller (PM 2.5). They found that personal outdoor, at home, exposures averaged 34% higher than was recorded by outdoor central monitors. The range of the personal exposures was 3.5–33.8 $\mu g/m^3$ of air, which was "likely due to local sources in communities" (Adgate *et al.*, 2002). Given the variability in exposures, we conservatively assume that exposure at an unfavorable location will increase the particle deposition dose by a factor of 2 over the particle size range considered.

To summarize the DEFs just considered, a very highly exposed individual in comparison to an average exposed one will have several characteristics: engaging in light exercise with oral breathing (DEF = 5), having severe COPD (DEF = 2), having anatomical/physiological predisposition to increased TB deposition (DEF = 2), and being exposed near local sources (DEF = 2). Although the likelihood of an individual possessing all these characteristics is unknown, it cannot be totally dismissed. Therefore, an extreme case of enhanced exposure could lead to $5 \times 2 \times 2 \times 2 = 40$-fold higher doses than those obtained for the average resting person. It should be noted that the selection of DEFs for our exposure scenario not only involves several assumptions and judgments but is also limited by the available data. Nevertheless, it is instructive to perform such dose estimates in order to formulate particle dosing strategies for *in vitro* toxicology studies.

Using the foregoing information, particle dosimetry calculations can be performed and the implications for cell culture studies noted.

RESULTS

Scenario 1

The first scenario, an average, resting, nose breathing, healthy adult, provides the particle deposition data shown in Table 1. For the calculations, MPPD1 was used with the following input values: Yeh and Schum geometry, 500-ml tidal volume, 12 breaths/min, nasal breathing, and no inhalability adjustment. The assumed environmental particle concentration is 100 $\mu g/m^3$, and the exposure duration is 2 h.

Therefore, in order to simulate the average surface deposition of particles in the size range considered, confluent epithelial cell cultures could logically be dosed with $1.7–3.4 \times 10^{-3}$ μg particles/cm^2 of culture surface. In this case, the particles would be added uniformly to the cell culture.

Scenario 2

The second scenario takes into account areas of high local particle deposition within the normal TB tree. The exposure scenario is the same as that for the first scenario, but local deposition on a region measuring 0.1 × 0.1 mm will be considered. This region, which comprises about 200 epithelial

TABLE 1
Total and Surface Particle Depositions for Scenario 1 at Resting Ventilation

Particle aerodynamic diameter (μm)	% TB deposition	Total TB deposition (μg)	TB surface deposition ($\mu g/cm^2$)
1	5.9	4.25	1.73×10^{-3}
2	8.6	6.19	2.51×10^{-3}
5	1.6	8.35	3.38×10^{-3}

TABLE 2
Surface Particle Depositions at TB Bifurcations for Scenario 2 at Resting Ventilation

Particle aerodynamic diameter (μm)	EF	TB surface deposition (μg/cm^2)
1	107	0.185
2	110	0.276
5	115	0.389

cells, will be located at the centers of the TB bifurcations, where the highest particle deposition will occur. Balásházy *et al.* (2003) performed CFD calculations for a minute volume of 5 l over the particle diameter range of 0.001–20 μm. Their results will be used in Table 2. EFs were actually read from Figure 4 in the cited reference, so they are within three EF units. For convenience, it is assumed that all TB bifurcations are equal with respect to the EFs.

In this case, *in vitro* surface particle depositions more than 100-fold above those for Scenario 1 could be justified. If the confluent cell culture had a total surface area of 1 cm^2 (100 mm^2), then particle doses ranging from about 0.2 to 0.4 μg/cm^2 could be considered as representing the highest-exposed cells in the human TB region. However, the particle exposure in the TB tree is local, in that the heavy deposits are surrounded by underexposed areas, and the TB bifurcations are separated by an average distance of about 2 mm (Yeh and Schum, 1980). Therefore, another method for applying particles to a 1 × 1-cm culture might be to separate 1-mm^2 deposits by 2 mm, which would appear as 25 equidistant applications as shown schematically in Figure 1. When adding particles in discrete deposits, investigators might consider first mixing the particles into a culture medium in order to prevent unwanted spreading of the dose.

If the minute volume is increased to 30 l (which occurs during light exercise), the EFs are generally greater than those at rest, as shown in Table 3 (Balásházy *et al.*, 2003).

The values for TB surface depositions in Table 3 are significantly larger than those in Table 2 for several reasons. First, oral breathing was assumed for Table 3, which modified the TB deposition fractions. Second, the increased ventilation in exercise for Table 3 is fivefold greater than at rest, which leads to greater deposition. Third, the EFs are different in exercise when compared to a resting state.

Scenario 3

The third and most complex scenario involves a consideration of the high-risk/high-dose individual who receives particle doses that are much greater than those for the average person. Table 4 presents the particle deposition–related factors of the high-dose individual in comparison to the average individual. The anatomy factor is taken from Lippmann (1977), and the exposure factor is taken from Adgate *et al.* (2002).

Using data from Table 4 and the TB particle depositions for oral breathing in exercise, Table 5 presents the dose calculations. MPPD1 was used with the following input values: Yeh and Schum geometry, 666.7-ml tidal volume, 45 breaths/min, oral breathing, and no inhalability adjustment.

The effects of exercise, oral breathing, lung disease, unusual anatomy, and proximity to particle sources produce calculated TB surface doses that exceed those of the average resting person by factors of about 33–67, depending on the particle size.

In order to calculate particle deposition doses to the most highly exposed TB epithelial cells, the EFs in Table 3 are combined with the surface doses in Table 5. The results, which provide surface doses in the local hot spots, are presented in Table 6.

As shown in Table 6, the most highly exposed TB cells in the high-dose individual are greater by approximately 3000–25,000 times than particle doses averaged over the TB region of the average individual. Although these results are striking, they are supported by quantitative dosimetric calculations.

DISCUSSION

Before discussing the limitations and potential applications of the dosimetry calculations, it is useful to present an

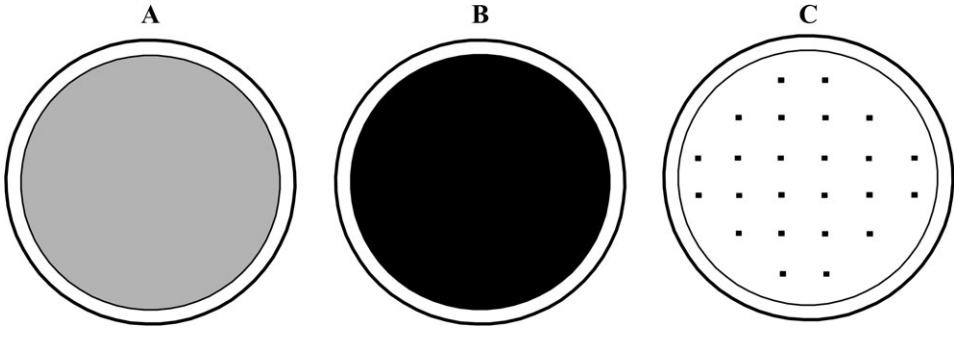

FIG. 1. Alternative methods for applying particles to TB cell cultures. (A) Uniform average particle exposure, as for Scenario 1. (B) Uniform exposure that represents most highly exposed cells, as in Scenario 2. (C) Focal particle exposure representing highly exposed cells surrounded by unexposed cells *in vivo*. For 5 μm particles inhaled by a healthy adult at rest, the particle doses/cm^2 of cell culture would be (A) 3.38×10^{-3}, (B) 0.389, and (C) 0.389 in each exposed area. Squares representing dosed regions cover approximately 200 cells. Not to scale.

TABLE 3
Surface Particle Depositions in the TB Region for Scenario 2 at an Exercising Ventilation

Particle aerodynamic diameter (μm)	EF	TB surface deposition (μg/cm^2)
1	80	0.629
2	190	1.938
5	380	10.69

equation that can be used to calculate surface deposition doses for aerosol particles.

$$\textit{In vitro}\ \text{particle concentration}\ (\text{mass}/\text{area}) = \frac{C \cdot V \cdot E_{\text{dep}} \cdot T_{\text{exp}} \cdot \text{EF}}{\text{VF} \cdot S},$$

where C = concentration of particles in environmental air (mass/volume), V = ventilation rate (volume/time), E_{dep} = deposition efficiency in the region of respiratory tract of interest, T_{exp} = duration of exposure (time), EF = EF at local deposition sites, VF = fraction of respiratory tract that is ventilated, which is diminished in some disease conditions, and S = surface area of the respiratory tract region of interest (area).

The values for variables in this equation are obtained from the literature and from particle deposition software, as previously noted. For Table 1, the equation used is as follows:

$$\textit{In vitro}\ \text{particle concentration}\ (\text{mass}/\text{area}) = \frac{C \cdot V \cdot E_{\text{dep}} \cdot T_{\text{exp}}}{S}.$$

For Tables 2 and 3, the added EF is from Balásházy *et al.* (2003).

For Tables 4 and 5, the equation used is as follows:

$$\textit{In vitro}\ \text{particle concentration}\ (\text{mass}/\text{area}) = \frac{C \cdot V \cdot E_{\text{dep}} \cdot T_{\text{exp}}}{\text{VF} \cdot S}.$$

For Table 6, the complete equation is used:

$$\textit{In vitro}\ \text{particle concentration}\ (\text{mass}/\text{area}) = \frac{C \cdot V \cdot E_{\text{dep}} \cdot T_{\text{exp}} \cdot \text{EF}}{\text{VF} \cdot S}.$$

There are many limitations associated with this dosimetry exercise, including key assumptions that were made, selection of the data used, consideration of only two dosing strategies (average or focal particle doses), selection of insoluble particles all of one size, not considering particle clearance effects, and considering only the TB region (and only epithelial cells in that region) of the respiratory tract. At this time, particle dose distributions for other cells, such as type I alveolar cells or macrophages, are difficult to calculate. Perhaps the major limitation is the assumption that each of the dose-enhancing factors is independent. For example, we have assumed that it is possible for an individual with substantially uneven ventilation and unusually high TB deposition efficiency to perform light exercise for 2 h at a substantially particle-polluted location. Admittedly, this is not a common scenario. In addition, we have assumed that the EFs for local cell populations arrived at by CFD modeling are realistic. Yet, as previously discussed, the CFD predictions are supported by data from hollow models and excised lungs. The values used for TB surface area, uneven ventilation in lung disease, and environmental particle concentrations were selected from many possible choices in the interest of limiting the paper's scope. With respect to environmental particle concentrations, 100 μg/m^3 in ambient air is high for general population exposures (but not for industrial exposures), but it was selected to keep the result values easy to visualize. If 1 μg/m^3 is more reasonable for a particular study, e.g., the surface doses can be divided by 100. The dosimetry calculations only took into account monodisperse, insoluble particles, which are idealizations of those found in the environment. Particle dispersion (as represented by the geometric standard deviation [GSD] for log-normally distributed particles) has an effect on the dose calculations. Although the

TABLE 4
Comparison of Particle Deposition–Related Factors for the Average and the High-Dose Individual

Individual	Ventilation (l/min)	Breathing mode	TB surface exposed (cm^2)	Anatomy factor[a]	Exposure factor[b]
Average	6	Nasal	2471	1	1
High dose	30	Oral	1235	2	2

[a]The anatomy factor represents possession of airway sizes and shapes that double the TB deposition in high-dose individuals.

[b]The exposure factor expresses exposure near particle sources, which also doubles the TB particle deposition.

TABLE 5
Particle Deposition Results for the High-Risk/High-Dose Individual without Inclusion of the EFs in Table 3

Particle aerodynamic diameter (μm)	% TB deposition	Total TB deposition (μg)	TB surface deposition (μg/cm^2)	Fold increase over average individual
1	5.4	77.8	0.063	36.6
2	7.0	101	0.082	32.5
5	19.3	278	0.225	66.6

TABLE 6
TB Surface Dose Estimated Combining Scenarios 2 and 3 and Comparison to Scenario 1

Particle aerodynamic diameter (μm)	EF	Average TB surface dose (μg/cm^2)	Enhanced TB surface dose (μg/cm^2)	Fold increase over Scenario 1
1	80	0.063	5.04	2913
2	190	0.082	15.58	6207
5	380	0.225	85.5	25,296

TABLE 7
Mass, Surface and Surface/Mass Values for Particles

Particle diameter (μm)	Particle mass (g)	Particle surface (cm^2)	Particle surface/mass (cm^2/g)
1	5.24×10^{-25}	3.14×10^{-16}	6×10^8
2	4.19×10^{-24}	1.26×10^{-15}	3×10^8
3	1.41×10^{-23}	2.83×10^{-15}	2×10^8
4	3.35×10^{-23}	5.03×10^{-15}	1.5×10^8
5	6.55×10^{-23}	7.85×10^{-15}	1.2×10^8
6	1.13×10^{-22}	1.13×10^{-14}	1×10^8
7	1.80×10^{-22}	1.54×10^{-14}	8.57×10^7
8	2.68×10^{-22}	2.01×10^{-14}	7.5×10^7
9	3.82×10^{-22}	2.54×10^{-14}	6.67×10^7
10	5.24×10^{-22}	3.14×10^{-14}	6×10^7

software used for calculating particle deposition (MPPD1) accepts a range of GSDs, the effect of GSD is not typically large. For example, for a 2-μm-diameter particle inhaled orally at rest, the TB deposition efficiency is 0.107 for a GSD = 1, 0.119 for a GSD = 1.5, and 0.142 for a GSD = 2. The deposition mechanism of interception was not considered, so the results do not apply to inhaled fibers. Because particle surface area has also been shown to relate to toxicity (Oberdörster, 2000), the airway surface doses may be multiplied by $6/\rho D$ (where ρ is particle density and D is particle diameter) to obtain doses in terms of particle surface to airway surface (cm^2/cm^2); Table 7 provides sample values.

Another limitation, ignoring the effect of particle clearance, was assumed for convenience and simplicity. However, the effect of TB clearance in a 2-h period is likely to be small, as the relatively complete clearance of particles from the TB region requires 1–2 days (NCRP, 1977, pp. 88–92), and cleared insoluble particles from more distal TB airways will enter more proximal airways (which compensates for local clearance). In any case, MPPD1 will accommodate particle clearance if one wishes to include it. If one were considering the upper airways (e.g., nose and throat) clearance rates would be an important factor. For the smallest airways (e.g., alveoli), the clearance rates for insoluble particles are slow (NCRP, 1977, pp. 92–95).

The scenarios considered only apply to adults, who have particle deposition values that are different from those of young children (Asgharian *et al.*, 2004; Phalen and Oldham, 2001; Yu and Xu, 1987). The respiratory disease considered in Scenario 2, COPD, was selected as values for uneven distribution of ventilation were available. If adequate data are available, other diseases can be modeled.

When applying our dosimetry calculations to *in vitro* studies, one must realize that neither the uniform particle depositions (Figs 1A and 1B) nor the equidistant focal depositions (Fig. 1C) actually occur in living lungs; the exposure patterns are more complex. Epithelial cells at the TB bifurcations receive large particle depositions that taper off with distance from the maximum point. Also, other regions of unusually high particle deposition in the TB region are seen in the CFD simulations. In addition, the spacing between bifurcations is much greater in large airways and smaller in the smallest airways than was assumed. Yet, practical considerations in applying particles to cell cultures prohibit the application of realistic distributions of particle deposits *in vivo*.

As can be seen from the foregoing discussion, our dosimetry modeling only crudely approximates the *in vivo* situation, but it is relevant to dosing cell cultures for toxicity evaluations (and possibly efficacy evaluations for inhaled medications).

CONCLUSIONS

This paper presented dosimetry calculations that are intended to guide *in vitro* toxicology studies that represent inhaled particles. The results imply that if local surface doses are considered, rather large particle exposures may occur. For high-dose individuals, the surface doses (representing maximally exposed groups of 200 TB epithelial cells) might be thousands of times greater than the corresponding surface doses averaged over the entire TB surface. The dosimetry calculations support the use of many, spaced focal particle applications, as opposed to uniform applications to cell cultures. However, the local doses calculated here are simplifications of *in vivo* dose distributions.

Finally, this paper presents some novel ideas related to applying particles to cell cultures. It is therefore important for others to perform similar dosimetry calculations in order to support, modify, or refute our results.

ACKNOWLEDGMENTS

The authors thank Susan Akhavan for administrative and editorial support. This research was supported by U.S. Environmental Protection Agency grant R827352 (Principal Investigator J. Froines of UCLA), as well as the U.S. Public Health Service (Principal Investigator A.Ncl, RO-1).

REFERENCES

Adgate, J. L., Ramachandran, G., Pratt, G. C., Waller, L. A., and Sexton, K. (2002). Spatial and temporal variability in outdoor, indoor, and personal PM2.5 exposure. *Atmos. Environ.* **36,** 3255–3265.

Asgharian, B., Menache, M. G., and Miller, F. J. (2004). Modeling age-related particle deposition in humans. *J. Aerosol Med.* **17,** 213–224.

Balásházy, I., and Hofmann, W. (1993). Particle deposition in airway bifurcations. 1. Inspiratory flow. *J. Aerosol Sci.* **24,** 745–772.

Balásházy, I., Hofmann, W., and Heistracher, T. (1999). Computation of local enhancement factors for the quantification of particle deposition patterns in airway bifurcations. *J. Aerosol Sci.* **30,** 185–203.

Balásházy, I., Hofmann, W., and Heistracher, T. (2003). Local particle deposition patterns may play a key role in the development of lung cancer. *J. Appl. Physiol.* **94,** 1719–1725.

Bell, K. A., and Friedlander, S. K. (1973). Aerosol deposition in models of a human lung bifurcation. *Staub Reinhalt. Luft* **33,** 178–182.

Bennett, W. D. (2000). How may the dosimetry of inhaled particles play a role in the observed mortality/morbidity associated with PM10? *Inhal. Toxicol.* **12**(Suppl. 1), 33–36.

Bennett, W. D., and Zeman, K. L. (2004). Effect of body size on breathing pattern and fine-particle deposition in children. *J. Appl. Physiol.* **97,** 821–826.

Bennett, W. D., Zeman, K. L., Kim, C., and Mascarella, J. (1997). Enhanced deposition of fine particles in COPD patients spontaneously breathing at rest. *Inhal. Toxicol.* **9,** 1–14.

Broday, D. M. (2004). Deposition of ultrafine particles at carinal ridges of the upper bronchial airways. *Aerosol Sci. Technol.* **38,** 991–1000.

Brown, J. S., Wilson, W. F., and Grant, L. D. (2005). Dosimetric comparisons of particle deposition and retention in rats and humans. *Inhal. Toxicol.* **17,** 355–385.

Centers for Health, Technology Transfer (CIIT) (2005). http://www.ciit.org/mppd/.

Chalupa, D. C., Morrow, P. E., Oberdörster, G., Utell, M. J., and Frampton, M. W. (2004). Ultrafine particle deposition in subjects with asthma. *Environ. Health Perspect.* **112,** 879–882.

Churg, A., and Vedal, S. (1996). Carinal and tubular airway particle concentrations in the large airways of non-smokers in the general population: Evidence for high particle concentration at airway carinas. *Occup. Environ. Med.* **53,** 553–558.

Cohen, B. S., Harley, N. H., Schlesinger, R. B., and Lippmann, M. (1988). Nonuniform particle deposition on tracheobronchial airways: Implications for lung dosimetry. *Ann. Occup. Hyg.* **32**(Suppl. 1), 1045–1053.

Gradón, L., and Orlicki, D. (1990). Deposition of inhaled aerosol particles in a generation of the tracheobronchial tree. *J. Aerosol Sci.* **21,** 3–19.

Heistracher, T., and Hofmann, W. (1997). Flow and deposition patterns in successive airway bifurcations. *Ann. Occup. Hyg.* **41,** 537–542.

Heyder, J., Gebhart, J., Stahlhofen, W., and Stuck, B. (1982). Biological variability of particle deposition in the human respiratory tract during controlled and spontaneous mouth-breathing. *Ann. Occup. Hyg.* **26,** 137–147.

Hofmann, W., Balásházy, I., Heistracher, T., and Koblinger, L. (1996). The significance of particle deposition patterns in bronchial airway bifurcations for extrapolation modeling. *Aerosol Sci. Technol.* **25,** 305–327.

Hofmann, W., Bergmann, R., and Balásházy, I. (2000). Variability and inhomogeneity of radon progeny deposition patterns in human bronchial airways. *J. Environ. Radioact.* **51,** 121–136.

International Commission on Radiation Protection, Task Group of Committee 2 (ICRP) (1994). *Human Respiratory Tract Model for Radiological Protection*, Publication 66. Pergamon Press, New York.

Ishikawa, Y., Nakagawa, K., Satoh, Y., Kitagawa, T., Sugano, H., Hirano, T., and Tsuchiya, E. (1994). "Hot spots" of chromium accumulation at bifurcations of chromate workers' bronchi. *Cancer Res.* **54,** 2342–2346.

Kaye, S. R., Phillips, C. G., and Winlove, C. P. (2000). Measurement of non-uniform aerosol deposition patterns in the conducting airways of the porcine lung. *J. Aerosol Sci.* **31,** 849–866.

Kim, C. S., and Kang, T. C. (1997). Comparative measurement of lung deposition of inhaled fine particles in normal subjects and patients with obstructive airway disease. *Am. J. Respir. Crit. Care Med.* **155,** 899–905.

Lippmann, M. (1977). Regional deposition of particles in the human respiratory tract. In *Handbook of Physiology—Reaction to Environmental Agents* (D. H. K. Lee, H. L. Falk, S. D. Murphy, and S. R. Geiger, Eds.), pp. 213–232. American Physiological Society, Bethesda, MD.

Martonen, T. B., Hofmann, W., and Lowe, J. E. (1987). Cigarette smoke and lung cancer. *Health Phys.* **52,** 213–217.

Mercer, R. R., Russell, M. L., Roggli, V. L., and Crapo, J. D. (1994). Cell number and distribution in human and rat airways. *Am. J. Respir. Cell Mol. Biol.* **10,** 613–624.

Miller, F. J., Anjilvel, S., Ménache, M. G., Asgharian, B., and Gerrity, T. R. (1995). Dosimetric issues relating to particulate toxicity. *Inhal. Toxicol.* **7,** 615–632.

National Council on Radiation Protection and Measurements (NCRP) (1997). *Deposition Retention and Dosimetry of Inhaled Radioactive Substances.* NCRP SC 57-2 Report. National Council on Radiation Protection and Measurements, Bethesda, MD.

Nowak, N., Kakade, P. P., and Annapragada, A. V. (2003). Computational fluid dynamics simulation of airflow and aerosol deposition in human lungs. *Ann. Biomed. Eng.* **31,** 374–390.

Oberdörster, G. (2000). Toxicology of ultrafine particles *in-vivo* studies. *Philos. Trans. R. Soc. Lond. Ser. A* **358,** 2719–2739.

Oldham, M., Phalen, R., and Heistracher, T. (2000). Computational fluid dynamic predictions and experimental results for particle deposition in an airway model. *Aerosol Sci. Technol.* **32,** 61–71.

Phalen, R. F., and Oldham, M. J. (2001). Modeling particle deposition as a function of age. *Respir. Physiol.* **128,** 119–130.

Schlesinger, R., Gurman, J., and Lippmann, M. (1982). Particle deposition within bronchial airways: Comparisons using constant and cyclic inspiratory flows. *Ann. Occup. Hyg.* **26,** 47–64.

Segal, R. A., Martonen, T. B., and Kim, C. S. (2000). Comparison of computer simulations of total lung deposition to human subjects data in healthy test subjects. *J. Air Waste Manage. Assoc.* **50,** 1262–1268.

Segal, R. A., Martonen, T. B., Kim, C. S., and Schearer, M. (2002). Computer simulations of particle deposition in the lungs of chronic obstructive pulmonary disease patients. *Inhal. Toxicol.* **14,** 705–720.

Sweeney, T. D., Skornik, W. A., Brain, J. D., Hatch, V., and Godleski, J. J. (1995). Chronic-bronchitis alters the pattern of aerosol deposition in the lung. *Am. J. Respir. Crit. Care Med.* **151,** 482–488.

Yeh, H. C., and Schum, G. M. (1980). Models of human lung airways and their application to inhaled particle deposition. *Bull. Math. Biol.* **42,** 461–480.

Yu, C. P., and Xu, G. B. (1987). Predicted deposition of diesel particles in young humans. *J. Aerosol. Sci.* **18,** 419–429.

Zhang, Z., Kleinstreuer, C., Donohue, J. F., and Kim, C. S. (2005). Comparison of micro- and nano-size particle depositions in a human upper airway model. *J. Aerosol Sci.* **26,** 211–233.

Zhu, Y., Hinds, W. C., Kim, S., and Sioutas, C. (2002). Concentration and size distribution of ultrafine particles near a major highway. *J. Air Waste Manage. Assoc.* **52,** 1032–1042.